Peptide OM-LV20 promotes structural and functional recovery of spinal cord injury in rats

Jian Zhao
Kunming Medical University
Ailang Pang
Kunming Medical University
Meifeng Yang
Kunming Institute of Zoology, Chinese Academy of Sciences
Xuemei Zhang
Kunming Medical University
Rong Zhang
Kunming Medical University
Jingfei Liu
Kunming Medical University
Yuanqi Gu
Kunming Medical University
Shanshan Li
Kunming Medical University
Saige Yin
Kunming Medical University
Yan Hu
Kunming Medical University
Due Zhang
Kunming Medical University
Yingchun Ba
Kunming Medical University
Buliang Meng
Kunming Medical University
Xinwang Yang (yangxinwanghp@163.com)
Faculty of Basic Medical Science, Kunming Medical University

Article

Keywords: Spinal cord injury, Peptides, Secondary injury, Neuroprotection, Motor function

Posted Date: February 22nd, 2021

DOI: https://doi.org/10.21203/rs.3.rs-258202/v1

Version of Record: A version of this preprint was published at Biochemical and Biophysical Research Communications on February 1st, 2022. See the published version at https://doi.org/10.1016/j.bbrc.2022.02.017.

Abstract

At present, there are no satisfactory therapeutic drugs for the functional recovery of spinal cord injury (SCI). We previously identified a novel peptide (OM-LV20) that accelerated the regeneration of injured skin tissues of mice and exerts neuroprotective effects against cerebral ischemia/reperfusion injury in rats. Here, the intraperitoneal injection of OM-LV20 (1 μg/kg) markedly improved motor function recovery in the hind limbs of rats with traumatic SCI, and further enhanced spinal cord repair. Administration of OM-LV20 increased the number of surviving neuron bodies, as well as the expression levels of brain-derived neurotrophic factor and its receptor tyrosine receptor kinase B. In the acute stage of SCI, OM-LV20 treatment also increased superoxide dismutase and glutathione content but decreased the levels of malonaldehyde and nitric oxide. Thus, OM-LV20 significantly promoted structural and functional recovery of SCI in adult rats by increasing neuronal survival and BDNF and TrkB expression, and thereby regulating the balance of oxidative stress. Based on our knowledge, this research is the first report on the effects of amphibian-derived peptide on the recovery of SCI and our results highlight the potential of peptide OM-LV20 administration in the acceleration of the recovery of SCI.

1. Introduction

Traumatic spinal cord injury (SCI) often results in severe nerve defects and dysfunction due to secondary injury and limited self-repair ability of the central nervous system. Patients with SCI often have different degrees of motor, sensory, and autonomic dysfunction. In severe cases, respiratory, urinary, and other systems may be affected, which can be life-threatening. These factors not only result in serious physical and psychological harm but can also cause huge economic burden to the patients, their families, and society as a whole [1]. The total global incidence of traumatic SCI is 10.5 cases per 100 000 people, reaching as high as 13.69 cases per 100 000 people in high-income countries, and the incidence rate continues to increase year by year [2,3].

After SCI, a series of primary and secondary pathological changes, such as ischemia and anoxia, electrolyte changes, free radical production, and lipid peroxidation, lead to neuronal apoptosis and necrosis, axon dissolution, and excessive microglia and astrocyte activation [4]. In the acute phase of injury, high inflammatory cell infiltration leads to a continuous inflammatory response and increased oxidative stress, which aggravate tissue damage and further deteriorate the structure and function of the spinal cord after injury [5]. Therefore, it is important to reduce secondary injury and improve the local microenvironment to promote function and circuit reconstruction after SCI [6]. At present, however, there is no specific drug treatment to solve these issues. The steroid drug methylprednisolone (MPED), which is widely used in the treatment of SCI, exhibits a better anti-inflammatory effect when used in large doses in the early stage of injury, but its side effects and therapeutic results have been questioned[7]. Therefore, the development of new drugs to promote SCI repair and recovery is critical.

Many peptides demonstrate high activity, high specificity, safety, low cost, and easy production [8]. A growing number of pharmacologically active peptides have also been identified, including antimicrobial [9], antioxidant [10], analgesic [11], wound-healing [12], and anti-gout peptides [13]. We previously identifified a peptide OM-LV20 (amino acid sequence: LVGKLLKGAVGDVCGLLPIC) from amphibian skin secretions, and functional results indicated that OM-LV20 accelerated the recovery of skin and regulated the levels of blood glucose in mice [14,15]. At the same time, our previous research found that peptide OM-LV20 exerts neuroprotective effects on cerebral ischemia reperfusion injury in rats. meanwhile, indicated that OM-LV20 had high stability and could through the MCAO-damaged blood-brain barrier[16]. Thus, based on the activities and characteristics of OM-LV20 and the pathological changes experienced in SCI, we applied this peptide for SCI treatment in adult Sprague-Dawley (SD) rats. Results showed that the application of OM-LV20 improved the microenvironment of the injured spinal cord and promoted motor function recovery of the hind limbs. Therefore, this study confirmed that natural active peptides could be used in the treatment of traumatic SCI, thus providing a new template for the development of candidate drugs to promote SCI repair.

2. Materials And Methods

2.1. Synthesis of OM-LV20

OM-LV20 has an amino acid sequence of 'LVGKLLKGAVGDVCGLLPIC' and an intramolecular disulfide bridge between 14th C and 20th C. OM-LV20 was artificially synthesized using solid phase synthesis and commercially provided by Wuhan Bioyeargene Biotechnology Co. Ltd. (Wuhan, China).

2.2. Animals

The adult SD rats (female, 230–250 g, 8–9-weeks old) used in this study were provided by the Animal Experimental Center of Kunming Medical University. The rats were housed individually in cages with free access to water and food. The animals were acclimatized to the environment for 7 days prior to surgery.

All animal experimental procedures were approved by the Institutional Animal Care and Use Committee of Kunming Medical University, China (SYXK (Yunnan) K2015-0002).

2.3. Construction of animal model of SCI

The rat SCI model was constructed according to a previous report [17]. Briefly, rats were randomly divided into normal (n = 6), sham-operated (n = 3), saline (n = 25), MPED (30 mg/kg,n = 25), OM-LV20 (10 ng/kg, n = 25), OM-LV20 (100 ng/kg, n = 25), and OM-LV20 groups (1 μg/kg, n = 25). Rats in the normal group had no SCI and received no drug intervention. Rats in the other five groups were anesthetized with pentobarbital sodium (50 mg/kg, intraperitoneal (i.p.) injection), after which the dorsal skin hair was shaved and bodies were fixed in a prone position under a surgical microscope (Olympus, SZ51, Japan). The surgical procedures have been described in detail in previous research [18]. In brief, the spinal cord was completely transected at thoracic level Th10. When the spinal cord was fully exposed, it was hooked with a blunt hook needle and cut with ophthalmic scissors. Transection was repeated three times on the cross-

section with a scalpel to ensure that the spinal cord was completely transected. For the sham-operated group, only the vertebral arch plate was opened. After the operation, the wound was locally coated with penicillin sodium powder. After the rats awakened, they received a dose of penicillin sodium (40 U/kg, intramuscular (i.m.) injection) twice a day until there was no hematuria.

2.4. Postoperative care and treatment

After surgery, all rats were maintained in single cages in a SPF feeding room and were cared for by nursing staff.

The bladder was emptied manually thrice a day until the voiding reflex was re-established. The MPED group received an i.p. injection once every 8 h after surgery (three times). The OM-LV20 and saline groups received i.p. administration once a day for 14 days after surgery.

2.5. Behavioural assessment

The Basso-Beattie-Bresnahan (BBB) scale was applied to evaluate the recovery of motor function of the hind limbs in rats. Briefly, three specially trained raters conducted double-blind evaluation on the day of surgery (after waking) and 3 days, 1 week, 2 weeks, 3 weeks, and 4 weeks after surgery. The rats were placed on an open scoring site and allowed to move freely for 5 min. The raters observed the rats and then evaluated their performance according to the BBB scale [19].

2.6. Histological evaluation

Four weeks after surgery, rats were euthanized with sodium pentobarbital (200 mg/kg, i.p.) and perfused intracardially with 200 mL of 0.9% saline, followed by 250 mL of 4% paraformaldehyde. Taking the injured site as the center, 2 cm of intact spinal cord was left at the head and tail, respectively, and photos were taken. After fixation and dehydration, frozen embedding methods were used to embed the spinal cord tissue and store in -80 ℃ refrigerator for future use.

2.7. Hematoxylin and eosin (H&E) staining

Spinal cord tissue was cut into 8-μm thick sections along the coronal plane, then stained with H&E. The staining results were observed and photographed using a microscope, and the tissue defect degree was analyzed by Image J [20].

2.8. Nissl staining

Spinal cord tissue was cut into 8-μm thick sections along the horizontal plane of the caudal end of the glial scar and the coronal surface of the injury site. The sections were then attached to glass slides, followed by Nissl staining (Solarbio, G1430, China), absolute ethanol dehydration, xylene transparency, and neutral gum sealing. The staining results were observed and photographed under a microscope, and the survival of neuronal cells was analyzed using Image J [21].

2.9. Immunohistochemical staining

Spinal cord tissue was cut into 8-μm thick sections along the coronal plane. The sections were attached to glass slides, Rinse in distilled water, soak in PBS for 5 minutes, incubate in 3% H2O2 deionized water for 15–20 minutes to eliminate endogenous peroxidase activity, rinse in PBS, 3 times, 3 minutes each

time, add blocking solution (20% normal goat serum)), incubate at room temperature for 15–20 minutes, pour off, drop primary antibodies, overnight at 4ºC, rinse with PBS, 3 times, 3 minutes each time, drop polymer adjuvant, incubate at 37°C for 15–20 minutes, rinse with PBS, 3 times, 3 minutes each time, drop horseradish enzyme labeled anti-rabbit IgG polymer, incubate at 37 ºC for 15–20 minutes, rinse with PBS, 3 times, 3 minutes each time, stained with DAB, washed with distilled water, counterstained with hematoxylin, dehydrated, transparently mounted, and sealed with neutral gum. The primary antibodies used for BDNF and TrkB were anti-BDNF rabbit pAb (1:150, Affinity Biosciences, DF6387, China) and anti-TrkB rabbit pAb (1:200, Proteintech, BC031835, China), respectively. A rabbit SP kit (SP-0023, Bioss, China) was used for secondary antibody detection. The staining results were observed and photographed under a microscope, and analyzed with Image J [21].

2.10. Enzyme-linked immunosorbent assay (ELISA)

Four weeks after surgery, rats were euthanized with sodium pentobarbital (200 mg/kg, i.p.) and perfused intracardially with 200 mL of 0.9% saline. The rats were then immediately placed on ice to remove the tissues of interest. With the injured site at the center, 1 cm of complete spinal cord was removed at the head and tail ends, respectively, then washed with precooled PBS (0.01 M, pH = 7.4) to remove residual blood clots, weighed, placed in sterile enzyme-free centrifuge tubes, and stored at − 80 ℃. The stored spinal cord tissues were then examined using a BDNF enzyme-linked immunosorbent kit (Jiang Lai Bio, JL12910, China). The Excel program was used to draw a standard regression curve and calculate the concentration of samples in different groups [21].

2.11. Determination of malondialdehyde (MDA), glutathione (GSH), superoxide dismutase (SOD), and nitric oxide (NOx) content

At 48 h after surgery, rats were anesthetized with pentobarbital sodium (200 mg/kg, i.p.), with 0.9% saline used for cardiac perfusion. The rats were then immediately placed on ice to collect the L-2 and S-1 spinal cord segment. The nerve root was cut and the spinal cord segment between L-2 and L-5 was preserved, with the tissue rinsed with prechilled PBS (0.01 M, pH = 7.4) to remove residual blood clots, then weighed, placed in sterile enzyme-free centrifuge tubes, and stored at − 80 ℃. The stored spinal cord tissues were then examined via relevant kits to determine MDA (Suzhou Grace Biotechnology Co. Ltd., G0109W, China), SOD (Suzhou Grace Biotechnology Co. Ltd., G0101W, China), GSH (Suzhou Grace Biotechnology Co. Ltd., G0206W, China), and NOx content (Suzhou Grace Biotechnology Co. Ltd., G0803W, China) [20].

3. Results

3.1. OM-LV20 significantly improved hind limb motor function in adult SD rats

During the 4-week observation period, the BBB scoring method was used to evaluate motor function recovery in SCI rats and number of deaths were also recoded. There were 6, 6, 10, 10, 10, 11, and 9 surviving rats in the normal, sham-operated, saline, MPED, OM-LV20 (10 ng/kg), OM-LV20 (100 ng/kg), and OM-LV20 (1 μg/kg) groups, respectively. The BBB scores are shown in Fig. 1A. From the operation to

4 weeks after, hind limb motor function in the SCI group recovered gradually, but not fully. In the first week after SCI, hind limb motor function in the OM-LV20 and MPED groups improved significantly compared with that in the saline group; at 4 weeks, the scores were 12.15 ± 1.88 for the saline group (n = 60), 12.88 ± 0.85 for the MPED group (n = 60), and 15.55 ± 1.23, 14.91 ± 1.98, and 15.56 ± 1.70 for the OM-LV20 groups (10 ng/kg, n = 60; 100 ng/kg, n = 66; 1 μg/kg, n = 54, respectively). The survival rates are shown in Fig. 1B. From days 3 to 14, some injured rats died due to infection, bowel obstruction, and sores. From day 14, the rats in each group passed the dangerous period, and the death rate decreased significantly, although the MPED group exhibited a significantly higher death rate than the other groups. At day 28, the survival rate in the MPED group was only 40.00%, whereas that in the saline group was 62.50%, OM-LV20 (10 ng/kg) group was 66.67%, OM-LV20 (100 ng/kg) group was 68.75%, and OM-LV20 (1 μg/kg) group was 69.23%. The percentage change in postoperative body weight is shown in Fig. 1C. After the operation, the body weights in each group decreased, with the MPED group showing the greatest loss.

3.2. OM-LV20 significantly reduced secondary injury of spinal cord tissue

Four weeks after surgery, the head and tail of the transected spinal cord grew together, and an obvious glial scar was observed (Fig. 2). However, the continuity of the two ends of the glial scar in the saline group was significantly worse than that in the OM-LV20 and MPED groups, and the glial scar in the saline group was significantly longer. As shown in Fig. 2A, obvious glial scars formed in each group and obvious defects remained in the tail of the glial scars in the saline group (shown by the blue arrow). Figure 2B shows the lengths of the local glial scars in each group, which were 8.50 ± 1.06 mm in the saline group (n = 4), 6.11 ± 1.14 mm in the MPED group (n = 7), 5.09 ± 0.73 mm in the OM-LV20 (10 ng/kg) group (n = 9), 5.26 ± 0.82 mm in the OM-LV20 (100 ng/kg) group (n = 5), and 5.38 ± 0.87 mm in the OM-LV20 (1 μg/kg) group (n = 10). We speculate that application of OM-LV20 might reduce secondary injury of spinal cord tissue in the acute phase and improve nerve cell survival at the injured site. This speculation was confirmed in the follow-up H&E staining and acute phase biochemical testing results.

3.3. OM-LV20 significantly promoted tissue regeneration at site of SCI

From the H&E staining results (Fig. 3), at 4 weeks after surgery, obvious tissue defects were observed in the injured areas in all groups. Compared with the saline group, however, the density of nerve fibers and cells in the OM-LV20 and MPED groups increased significantly. Figure 3B shows the tissue defects in the glial scar region in each group, with a tissue defect rate of 36.84% ± 3.97% in the saline group (n = 9), 24.55% ± 4.84% in the MPED group (n = 9), 26.84% ± 2.35% in the OM-LV20 (10 ng/kg) group (n = 9), 24.17% ± 4.79% in the OM-LV20 (100 ng/kg) group (n = 9), and 18.38% ± 4.02% in the OM-LV20 (1 μg/kg) group (n = 9).

3.4. OM-LV20 increased survival of neuronal cell bodies at injury site

Staining of the caudal area of the glial scars showed that there were fewer neuronal cell bodies in each group (Fig. 4); however, compared to the OM-LV20 and MPED groups, the number of neuronal cell bodies in the saline group decreased significantly (Fig. 4B, black arrow refers to neuronal cell bodies). Figure 4C shows the number of surviving neuronal cell bodies in each group, i.e., 6.22 ± 0.83 in the saline group (n = 9), 11.00 ± 1.12 in the MPED group (n = 9), 9.67 ± 1.23 in the OM-LV20 (10 ng/kg) group, 10.00 ± 1.41 in

the OM-LV20 (100 ng/kg) group, and 11.33 ± 1.80 in the OM-LV20 (1 μg/kg) group. The coronal surface staining is shown in Fig. 5. Results indicated that there were fewer neuronal cell bodies in the injured area; however, compared to the OM-LV20 and MPED groups, the number of neuronal cell bodies in the saline group decreased significantly (Fig. 5B, black arrow refers to neuronal cell bodies). Figure 5C shows the number of surviving neuronal cell bodies in each group, i.e., 0.78 ± 0.67 in the saline group (n = 9), 2.44 ± 0.73 in the MPED group (n = 9), 1.00 ± 0.71 in the OM-LV20 (10 ng/kg) group, 1.56 ± 0.56 in the OM-LV20 (100 ng/kg) group, and 2.67 ± 0.71 in the OM-LV20 (1 μg/kg) group. These results indicate that neurons showed good survival after treatment with the active peptide (OM-LV20) and MPED. Thus, survival status and number of neuronal cells are of great significance to functional recovery after SCI.

3.5. OM-LV20 increased expression of BDNF and its main receptor TrkB

The BDNF immunohistochemical staining results of the coronal surface of the spinal cord tissue are shown in Fig. 6A. As seen in Fig. 6B, expression of BDNF in the OM-LV20 and MPED groups increased significantly compared with that in the saline group, i.e., 6.33% ± 0.80% in the saline group (n = 9), 14.18% ± 3.24% in the MPED group (n = 9), 12.90% ± 1.35% in the OM-LV20 (10 ng/kg) group (n = 9), 14.28% ± 1.69% in the OM-LV20 (100 ng/kg) group (n = 9), and 17.34% ± 2.50% in the OM-LV20 (1 μg/kg) group (n = 9). These results are consistent with the detection of BDNF using ELISA. As shown in Fig. 6C, expression of BDNF in the OM-LV20 and MPED groups increased significantly compared with that in the saline group, i.e., 165.13 ± 10.41 in the saline group (n = 9), 206.55 ± 15.60 in the MPED group (n = 9), 179.29 ± 11.20 in the OM-LV20 (10 ng/kg) group (n = 9), 189.65 ± 23.10 in the OM-LV20 (100 ng/kg) group (n = 9), and 198.98 ± 15.69 in the OM-LV20 (1 μg/kg) group (n = 9). At the same time, we used immunohistochemical staining to detect the expression of TrkB (Fig. 7A). As shown in Fig. 7B, TrkB expression in the OM-LV20 and MPED groups increased significantly compared to that in the saline group, i.e., 7.34% ± 1.70% in the saline group (n = 9), 15.53% ± 2.37% in the MPED group (n = 9), 13.22% ± 1.17% in the OM-LV20 (10 ng/kg) group (n = 9), 14.58% ± 1.78% in the OM-LV20 (100 ng/kg) group (n = 9), and 15.69% ± 3.59% in the OM-LV20 (1 μg/kg) group (n = 9). These results indicate that the application of OM-LV20 can promote the expression of BDNF and its main receptor TrkB.

3.6. OM-LV20 improved microenvironment of acute stage SCI and reduced secondary injury of tissue

We measured SOD, MDA, GSH, and total NOx content in the spinal cord (between L-2 and L-5) 48 h after surgery (Fig. 8). As shown in Fig. 8A, SOD content was significantly higher in the OM-LV20 groups than that in the saline group, i.e., 276.10 ± 57.74 U/g protein in the saline group (n = 9), 519.46 ± 133.78 U/g protein in the MPED group (n = 9), 414.00 ± 123.08 U/g protein in the OM-LV20 (10 ng/kg) group (n = 9), 452.66 ± 122.44 U/g protein in the OM-LV20 (100 ng/kg) group (n = 9), and 554.35 ± 166.34 U/g protein in the OM-LV20 (1 μg/kg) group (n = 9). As shown in Fig. 8B, compared with that in the saline group, MDA content in the OM-LV20 groups was very low, i.e., 10.88 ± 3.53 nmol/g in the saline group (n = 9), 3.78 ± 1.42 nmol/g in the MPED group (n = 9), 9.08 ± 2.34 nmol/g in the OM-LV20 (10 ng/kg) group (n = 9), 4.16 ± 1.48 nmol/g in the OM-LV20 (100 ng/kg) group (n = 9), and 2.79 ± 1.47 nmol/g in the OM-LV20 (1 μg/kg) group (n = 9). As shown in Fig. 8C, GSH content was higher in the OM-LV20 groups than that in the saline group, i.e., 1.28 ± 0.20 μmol/g in the saline group (n = 9), 2.78 ± 0.86 μmol/g in the MPED group, 2.24 ± 0.45 μmol/g in the OM-LV20 (10 ng/kg) group (n = 9), 2.49 ± 0.37 μmol/g in the OM-LV20 (100

ng/kg) group (n = 9), and 2.95 ± 0.77 μmol/g in the OM-LV20 (1 μg/kg) group (n = 9). As shown in Fig. 8D, NOx content was significantly lower in the OM-LV20 groups compared with that in the saline group, i.e., 11.11 ± 3.11 nmol/min/g in the saline group (n = 9), 4.40 ± 1.01 nmol/min/g in the MPED group (n = 9), 8.03 ± 3.31 nmol/min/g in the OM-LV20 (10 ng/kg) group (n = 9), 7.46 ± 1.42 nmol/min/g in the OM-LV20 (100 ng/kg) group (n = 9), and 3.32 ± 1.52 nmol/min /g in the OM-LV20 (1 μg/kg) group (n = 9). Based on these four commonly used indicators, treatment with the active peptide OM-LV20 significantly improved the local microenvironment in the acute phase of SCI, which had important impact on secondary injury and recovery.

4. Discussion

We studied the effects of a natural active peptide on the recovery of spinal cord structure and function after acute SCI. We used behavioral scores, acute-phase biochemical tests, and pathological tests to study SCI recovery. Results showed that OM-LV20 had a positive effect on SCI repair, suggesting that the application of natural active peptides may have broad prospects for the treatment of SCI.

Here, OM-LV20 showed strong ability to promote repair in an acute wound repair model. Whether for skin trauma or acute SCI, several similarities in pathophysiology and repair conditions are found during the acute stage of injury, including activation of inflammatory cells, accumulation of toxic substances, generation of free radicals, and damage to the local microenvironment, which all have important effects on repair after injury [22,23]. In previous reports,intraperitoneal administration of OM-LV20 could signifificantly reduce the infarct area formation, protect cortical and hippocampal neurons from death in I/R rats. Moreover, the underlying molecular mechanism was partly involved with the regulation of the MAPK and BDNF/AKT signaling pathways, as well as TPH1, cAMP, and PAC1R levels[16]. The current research is based on the remarkable ability of OM-LV20 to promote skin injury repair and the neuroprotective effects.

The choice of injury model is important for studies on SCI. At present, the most commonly used models are acute spinal cord contusion, clamping compression injury, ischemic injury, and transected injury [24]. Here, we chose the complete spinal cord transected injury model [25]. Although this model exhibits high mortality and difficulty in nursing, it is one of the most effective models for SCI, and has great value in verifying dynamic changes in the microenvironment at the site of injury and restoration of spinal cord structure and function [26].

Lipid peroxidation is mediated by free radicals in the acute phase of SCI and has an important effect on secondary injury [27]. As the final product of lipid peroxidation, MDA levels can indirectly reflect the severity of acute phase cell injury [28]. Similarly, increases in NOx are often observed after injury, and can aggravate tissue damage [29]. Furthermore, both SOD activity [30] and GSH content can reflect the clearance of free radicals after injury [31]. Thus, these bioindicators can be used to judge the severity of SCI during the acute phase of injury. After the occurrence of SCI, the expression levels of BDNF and its receptor TrkB also

change significantly, and their presence is important for the survival and functional recovery of neuronal cells [32]. BDNF plays a biological role in the activation of full-length TrkB, and an important role in neuronal survival, axon damage, and nerve regeneration [33]. In the spinal cord of normal adult mammals, BDNF is almost undetectable. After SCI, however, BDNF and TrakB are highly expressed in the injured area [34]. In the early stage of injury, BDNF and TrkB are mainly synthesized by neurons and astrocytes; after the acute stage, however, they are mainly synthesized by microglia and macrophages [35]. BDNF and TrkB can help reduce primary injury, protect neuronal cells, and promote axon regeneration [34,36]. At the same time, BDNF can effectively increase the expression of heme oxygenase and heat shock protein in the injured area to reduce secondary injury after SCI. Here, after OM-LV20 treatment of SCI, the content of SOD and GSH in the local spinal cord tissue increased significantly, whereas the content of MDA and NOx decreased significantly. At the same time, the expression levels of BDNF and TrkB were effectively up-regulated, which improved the local microenvironment of the injured site and reduced secondary tissue injury. These favorable environments enhanced neuronal cell survival, with survival status and number of neuronal cells directly determining the degree of functional recovery after injury.

After the acute phase of SCI, a local glial scar gradually develops, which has a decisive role in the recovery of function following injury. After SCI, astrocytes in the damaged area will transform into reactive astrocytes, then mature into scar-like astrocytes, and eventually form a dense glial scar around the injured area. Although the scar tissue in the subacute phase can promote nerve regeneration to a certain extent, scar tissue in the late stage can hinder the regeneration of axons and recovery of spinal cord function, which is a common problem encountered in the treatment of SCI [37]. Scar tissue hinders the axons from crossing the injury site and affects the transmission of biological signals. Thus, the effective removal of old scar tissue should help restore sensory and motor functions after SCI [38]. Although the application of OM-LV20 failed to directly remove old scar tissue, the H&E results (Fig. 3) showed that the active peptide effectively reduced tissue defects at the injury site. More importantly, the old glial scar tissue in the OM-LV20 groups was significantly shorter than that in the saline group (Fig. 2), which may be an important reason for the significant improvement in hind limb motor function.

In summary, this study showed that the application of an active peptide in the treatment of SCI effectively improved the local microenvironment of the injury, and significantly enhanced the structure of the injured spinal cord and function of the hind limbs in rats. These findings provide strong support for the application of natural active peptides in the treatment of SCI and their use in the development of new drugs and multi-channel combined treatments.

Abbreviations

: SCI, spinal cord injury; BDNF, brain-derived neurotrophic factor; TrkB, tyrosine receptor kinase B; MPED, methylprednisolone; SD, Sprague-Dawley; BBB, Basso-Beattie-Bresnahan; H&E, Hematoxylin and eosin; ELISA, Enzyme-linked immunosorbent assay; MDA, Determination of malondialdehyde; GSH, glutathione; SOD, superoxide dismutase; NOx, nitric oxide.

Declarations

Consent for Publication

All authors agree to the publication of this paper.

Compliance with ethical standards

Required Author Disclosure Forms provided by the authors are available with the online version of this article.

Funding statement

This work was supported by grants from the National Natural Science Foundation of China (81760648 and 31670776), Yunnan Applied Basic Research Project-Kunming Medical University Union Foundation (2019FE001 (-162), 2019FE001 (-183), and 2019FE001 (-206)), and Applied Research Foundation of Diagnosis and Treatment Center of Nervous System Diseases of Yunnan Province (ZX2019-03-05).

Author contributions

B., B.M., and X.Y. acquired funding and designed the research. J.Z. and M.Y. performed most of the experiments. M.Y., X.Z., R.Z., J.L., and Y.G. assisted in the experiments. S.L., S.Y., Y.H. and Y.Z. analyzed the data. All authors contributed substantially to this research and reviewed the manuscript.

References

1 Donovan, J. & Kirshblum, S. Clinical Trials in Traumatic Spinal Cord Injury. *Neurotherapeutics* (2018).

2 Kumar, R. *et al.* Traumatic spinal injury: global epidemiology and worldwide volume. *World Neurosurgery*, S1878875018303036 (2018).

3 Lee, J. Y., Choi, H. Y. & Yune, T. Y. J. N. Fluoxetine and vitamin C synergistically inhibits blood-spinal cord barrier disruption and improves functional recovery after spinal cord injury. 78 (2016).

4 Sundgren, P. C. & Flanders, A. E. Spinal Trauma and Spinal Cord Injury. (2016).

5 Zhijiang *et al.* An anti-inflammatory peptide and brain-derived neurotrophic factor-modified hyaluronan-methylcellulose hydrogel promotes nerve regeneration in rats with spinal cord injury. *International Journal of Nanomedicine* (2019).

6 Eckert, M. J. & Martin, M. J. Trauma. *Surgical Clinics of North America* **97**, 1031-1045, doi:10.1016/j.suc.2017.06.008 (2017).

7 Machova Urdzikova, L. *et al.* A green tea polyphenol epigallocatechin-3-gallate enhances neuroregeneration after spinal cord injury by altering levels of inflammatory cytokines. S0028390817304203 (2017).

8 Kaspar, A. A. & Reichert, J. M. Future directions for peptide therapeutics development. *Drug Discovery Today* **18**, 807-817 (2013).

9 Ren, L., Jian-Guo, L. & Yun, Z. Antimicrobial Peptides in Amphibian Skins and Their Application. *Zoological Research* (2004).

10 Yang, X., Wang, Y., Zhang, Y., Lee, W. H. & Zhang, Y. Rich diversity and potency of skin antioxidant peptides revealed a novel molecular basis for high-altitude adaptation of amphibians. *Scientific Reports* **6**, 19866 (2016).

11 Li, C. *et al.* Purification and function of two analgesic and anti-inflammatory peptides from coelomic fluid of the earthworm, Eisenia foetida. *Peptides* **89**, 71-81 (2017).

12 Song, Y. *et al.* A short peptide potentially promotes the healing of skin wound. *Bioscience Reports* (2019).

13 Naixin *et al.* A new rice-derived short peptide potently alleviated hyperuricemia induced by potassium oxonate in rats. *Journal of agricultural and food chemistry* (2018).

14 Li, X. *et al.* OM-LV20, a novel peptide from odorous frog skin, accelerates wound healing in vitro and in vivo. *Chemical Biology & Drug Design* **91**, 126-136, doi:10.1111/cbdd.13063 (2018).

15 Shang, W. *et al.* Characterization of an insulinotropic peptide from skin secretions of Odorrana andersonii. (2017).

16 Yin, S. *et al.* Peptide OM-LV20 exerts neuroprotective effects against cerebral ischemia/reperfusion injury in rats. **537**, 36-42 (2021).

17 Du, B. L. *et al.* Graft of the gelatin sponge scaffold containing genetically-modified neural stem cells promotes cell differentiation, axon regeneration, and functional recovery in rat with spinal cord transection. *Journal of Biomedical Materials Research Part A* **103**, 1533-1545 (2015).

18 Celichowski, J. *et al.* Changes in contractile properties of motor units of the rat medial gastrocnemius muscle after spinal cord transection. **91** (2010).

19 He *et al.* Transplantation of adult spinal cord grafts into spinal cord transected rats improves their locomotor function. *Science China(Life Sciences)* (2019).

20 Durdag, E., Yildirim, Z., Unlu, N. L., Kale, A. & Ceviker, N. Neuroprotective Effects of Vigabatrin on Cord Ischemia-Reperfusion Injury. *World Neurosurgery* **120** (2018).

21 Sun, L. *et al.* Co-Transplantation of Human Umbilical Cord Mesenchymal Stem Cells and Human Neural Stem Cells Improves the Outcome in Rats with Spinal Cord Injury. *Cell Transplantation* (2019).

22 Mcdonald, J. W. & Sadowsky, C. Spinal-cord injury. *Lancet* **359**, 417-425 (2002).

23 Bian, W., Meng, B., Li, X., Wang, S. & Yang, X. OA-GL21, a novel bioactive peptide from Odorrana andersonii , accelerated the healing of skin wounds. *Bioscience Reports* **38** (2018).

24 Becker, O. J. R. N. Animal models in spinal cord injury: a review. **19**, 47-60 (2008).

25 Fan, Z., Liao, X., Tian, Y., xuzhuzi, X. & Nie, Y. A prevascularized nerve conduit based on a stem cell sheet effectively promotes the repair of transected spinal cord injury. *Acta Biomaterialia* **101**, 304-313, doi:10.1016/j.actbio.2019.10.042 (2020).

26 Liu, Z. *et al.* Restoration of motor function after operative reconstruction of the acutely transected spinal cord in the canine model. *Surgery*, S0039606017307110 (2017).

27 Lim, P. A. C. & Tow, A. M. J. A. o. t. A. o. M., Singapore. Recovery and regeneration after spinal cord injury: A review and summary of recent literature. **36**, 49-57 (2007).

28 Ahadi, S., Zargari, M. & Khalatbary, A. R. Assessment of the neuroprotective effects of (-)-epigallocatechin-3-gallate on spinal cord ischemia-reperfusion injury in rats. *The journal of spinal cord medicine*, 1-8 (2019).

29 Maggio, D. M. *et al.* Acute Molecular Perturbation of Inducible Nitric Oxide Synthase with an Antisense Approach Enhances Neuronal Preservation and Functional Recovery after Contusive Spinal Cord Injury. *Journal of Neurotrauma* **29**, 2244-2249 (2012).

30 Ozturk *et al.* Epidermal growth factor regulates apoptosis and oxidative stress in a rat model of spinal cord injury. *Injury* (2018).

31 Sgaravatti, n. M. *et al.* Effects of 1,4-butanediol administration on oxidative stress in rat brain: Study of the neurotoxicity of γ-hydroxybutyric acidin vivo. *Metabolic Brain Disease* **24**, 271-282 (2009).

32 Han, D. *et al.* The Neuroprotective Effects of Muscle-Derived Stem Cells via Brain-Derived Neurotrophic Factor in Spinal Cord Injury Model. *Biomed Research International* **2017**, 1-11 (2017).

33 Diener, P. S. & Bregman, B. S. J. N. Neurotrophic factors prevent the death of CNS neurons after spinal cord lesions in newborn rats. **5**, 1913 (1994).

34 Bamber, N. I. *et al.* Neurotrophins BDNF and NT-3 promote axonal re-entry into the distal host spinal cord through Schwann cell-seeded mini-channels. *European Journal of Neuroscience* **13**, 257 (2001).

35 Ying *et al.* Trk A, B, and C are commonly expressed in human astrocytes and astrocytic gliomas but not by human oligodendrocytes and oligodendroglioma. (1998).

36 Condorelli, D. F. *et al.* Neurotrophins and theirtrk receptors in cultured cells of the glial lineage and in white matter of the central nervous system. **6**, 237-248 (1995).

37 Li, X., Yang, B., Xiao, Z., Zhao, Y. & Dai, J. Comparison of subacute and chronic scar tissues after complete spinal cord transection. *Experimental Neurology* **306**, 1-13 (2018).

38 Zhao, Y. *et al.* Clinical Study of NeuroRegen Scaffold Combined With Human Mesenchymal Stem Cells for the Repair of Chronic Complete Spinal Cord Injury. *Cell Transplantation* **26**, 891-900 (2017).

Figures

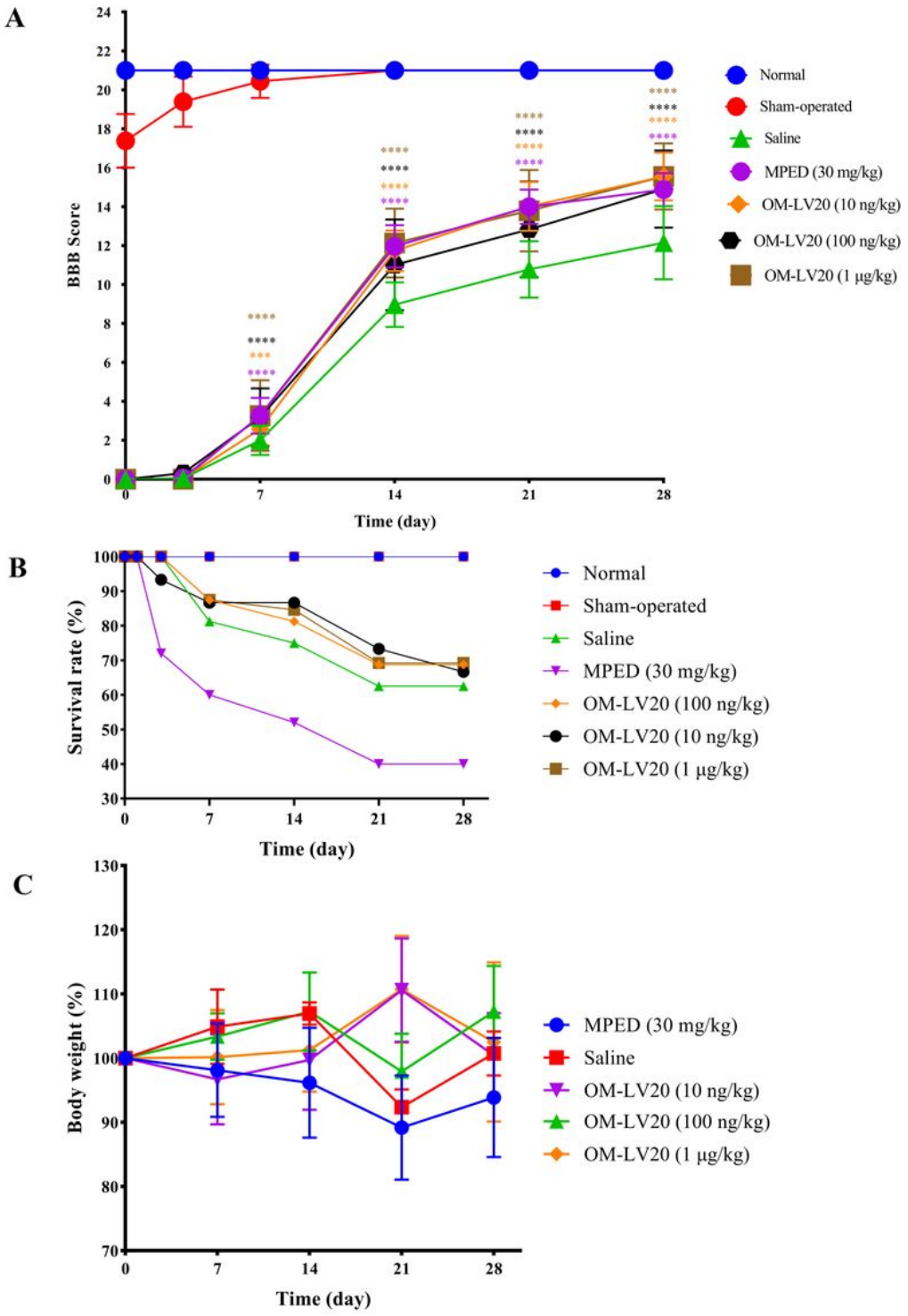

Figure 1

Behavioral evaluation of motor function of hind limbs, survival rate, and weight change in rats with total transverse spinal cord injury. A. BBB scores of rats in each group. During first week after surgery, scores of OM-LV20 groups were higher than that of saline group, with marked differences at 4 weeks, All data are means ± SD of three independent experiments performed in triplicate. *** $p < 0.001$; **** $p < 0.0001$. B. Survival percentage of rats in each group at day 28. Survival rate of MPED group was only 40%. C.

Percentage change in postoperative body weight. MPED group showed significant weight loss after surgery.

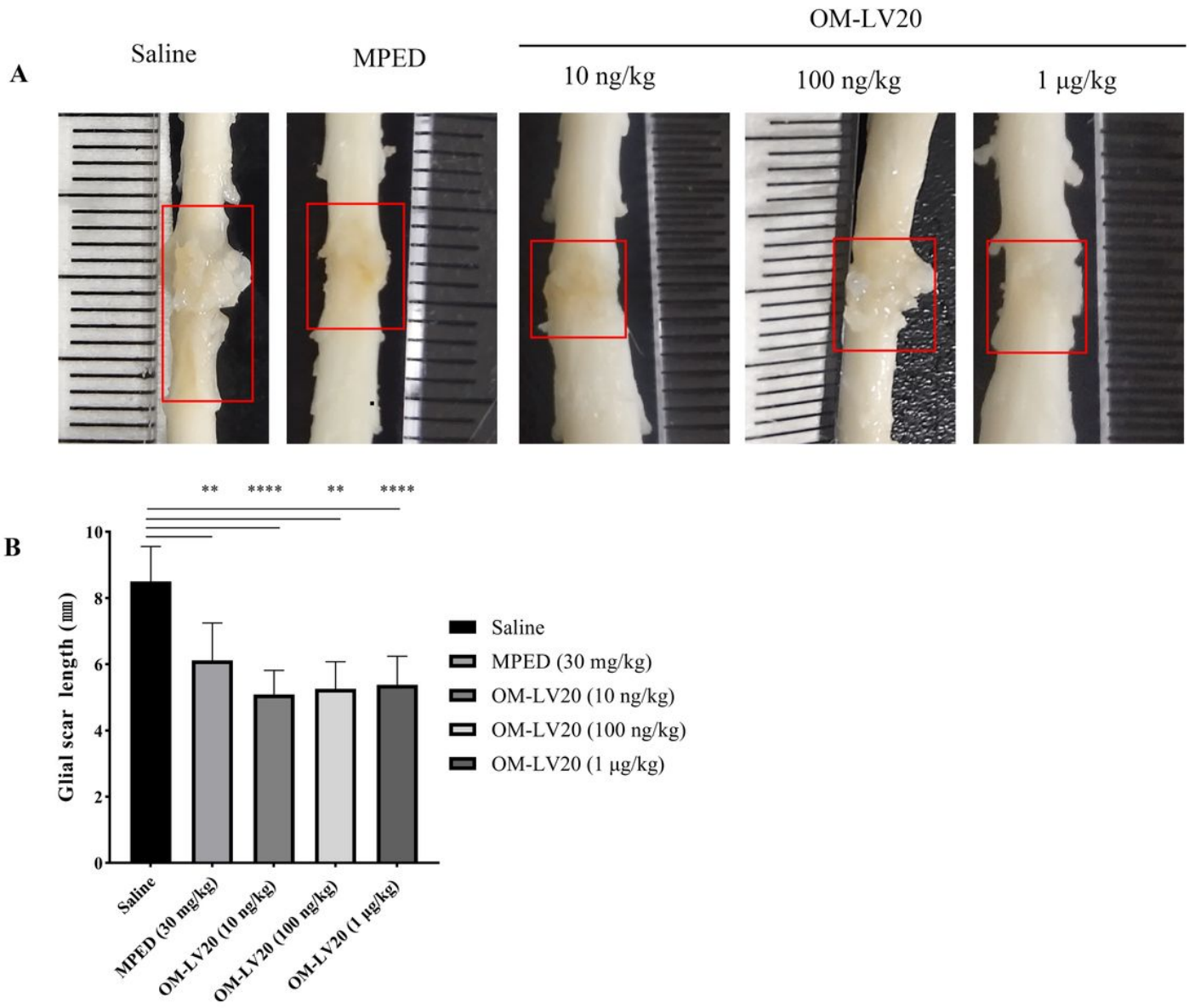

Figure 2

Dorsal side view and quantification of spinal cord injury site 4 weeks after surgery. A. Area of glial scar (red box) and caudal defect of glial scar in saline group (blue arrow). B. Quantification of glial scar length . ** Significifficant difffference at $p < 0.01$; **** $p < 0.0001$. All bars represent means ± SD from three diffferent sections for each experiment.

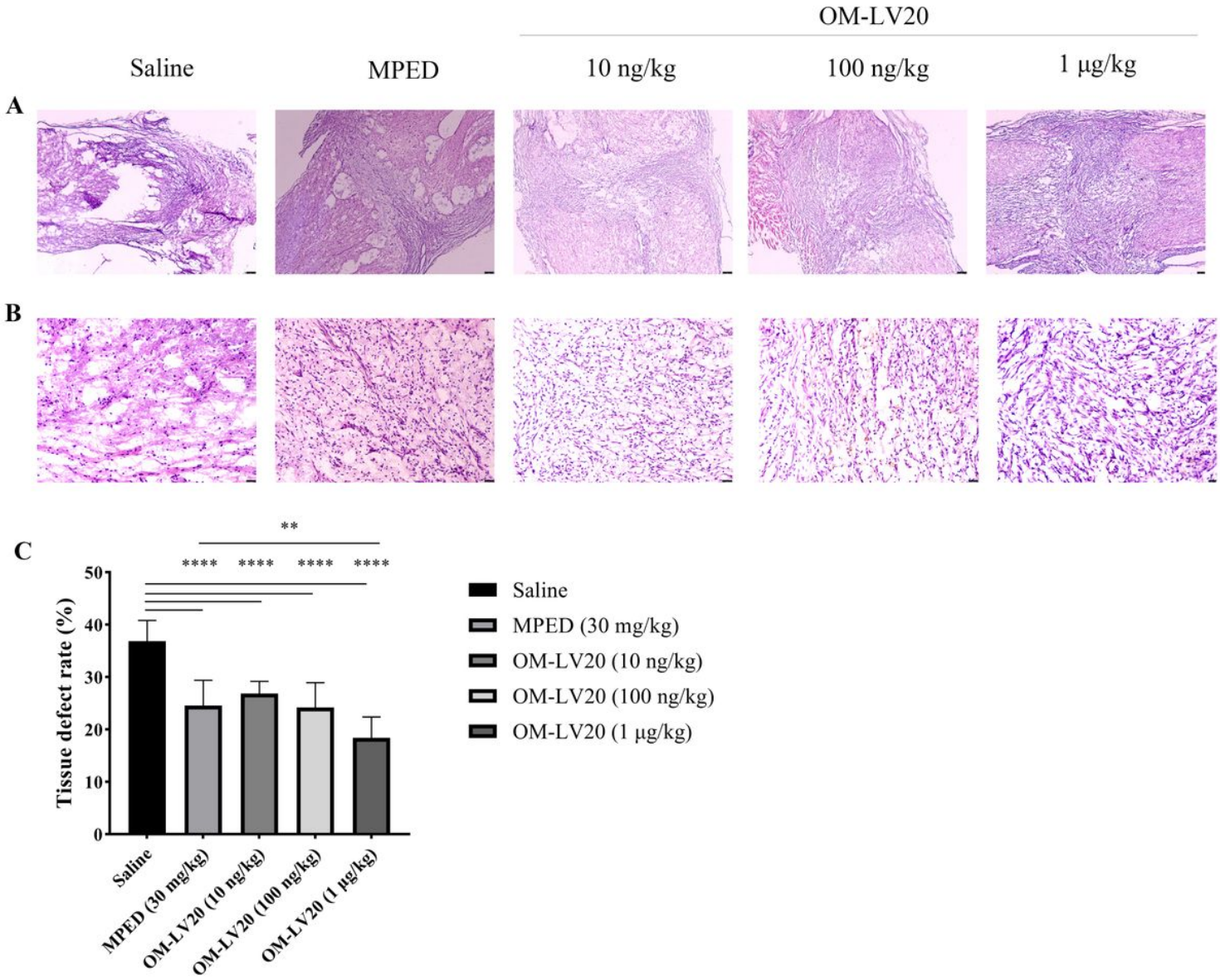

Figure 3

H&E staining and quantification of spinal cord injury 4 weeks after surgery. A. The samples were observed at 40× field-of-view magnification, black box is caudal side of glial scar. B. The samples were observed at 100 × field-of-view magnification. C. Quantification of tissue defects in glial scar area. Scale bar, 25 μm. ** Significant diffference at $p < 0.01$; **** $p < 0.0001$. All bars represent means ± SD from three diffferent sections for each experiment.

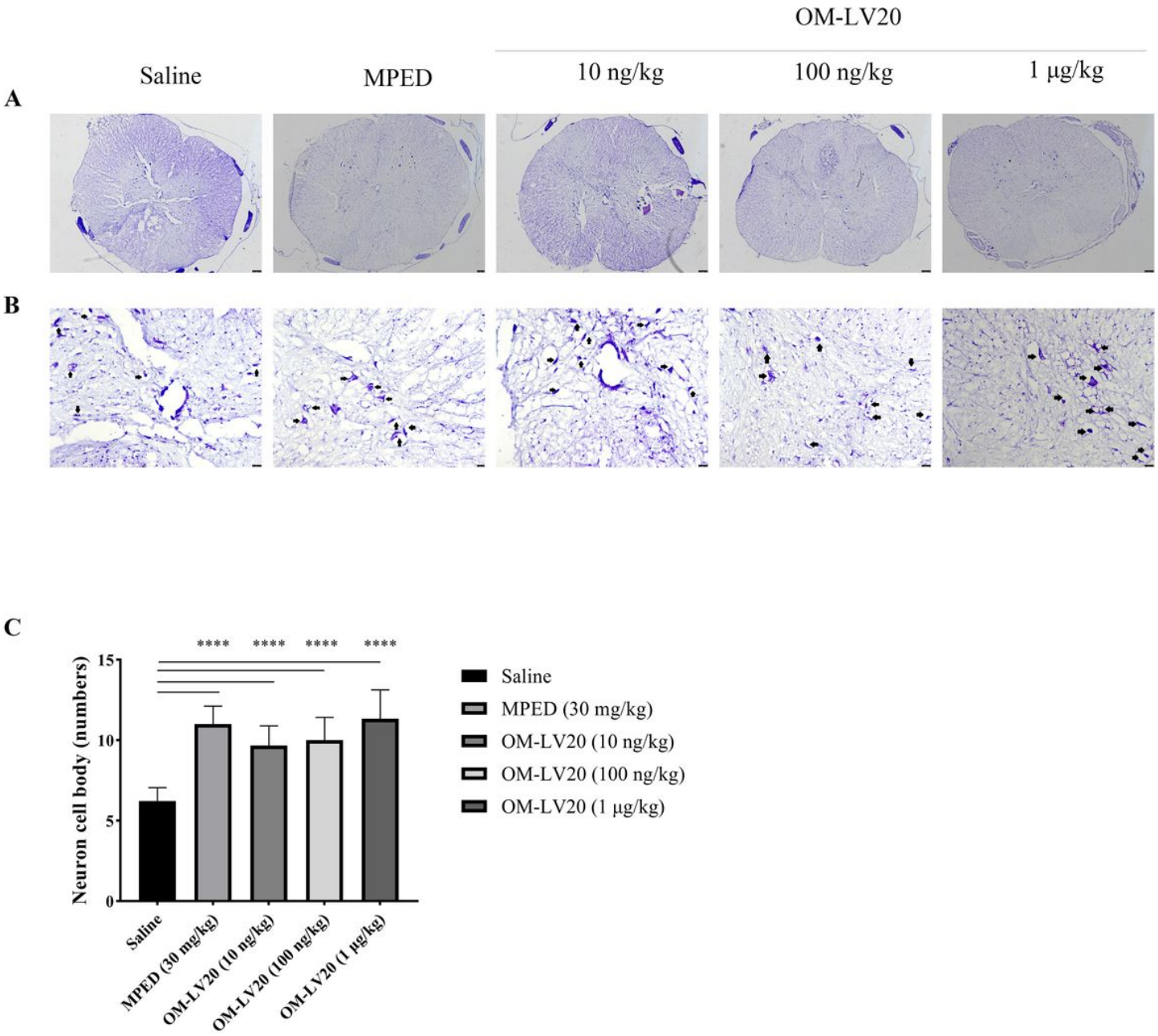

Figure 4

Nissl staining and quantification of caudal horizontal surface of glial scar in spinal cord injury 4 weeks after surgery. A. The samples were observed at 40 × magnifications. B. The samples were observed at 100 × field-of-view magnification. C. Number of neuronal cell bodies surviving on horizontal plane. Scale bar, 25 μm. **** Significant diffference at $p < 0.0001$. All bars represent means ± SD from three diffferent sections for each experiment.

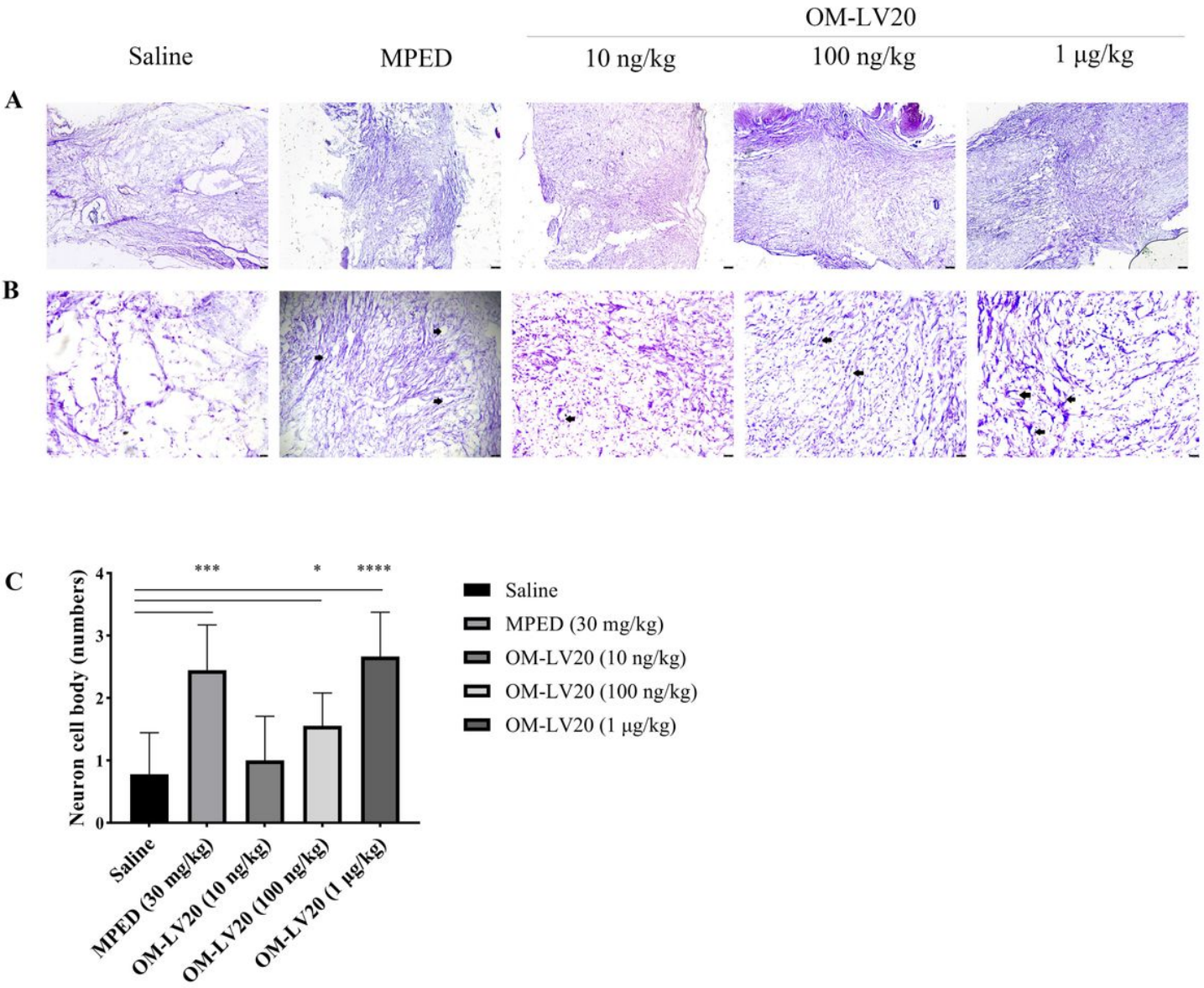

Figure 5

Nissl staining and quantification of coronary surface of glial scar in spinal cord injury 4 weeks after surgery. A. The samples were observed at 40 × magnifications. B. The samples were observed at 100 × magnifications. C. Number of neuronal cell bodies surviving on coronal plane. Scale bar, 25 μm. * Significifant diffference at $p < 0.05$; ***$p < 0.001$; **** $p < 0.0001$. All bars represent means ± SD from three diffferent sections for each experiment.

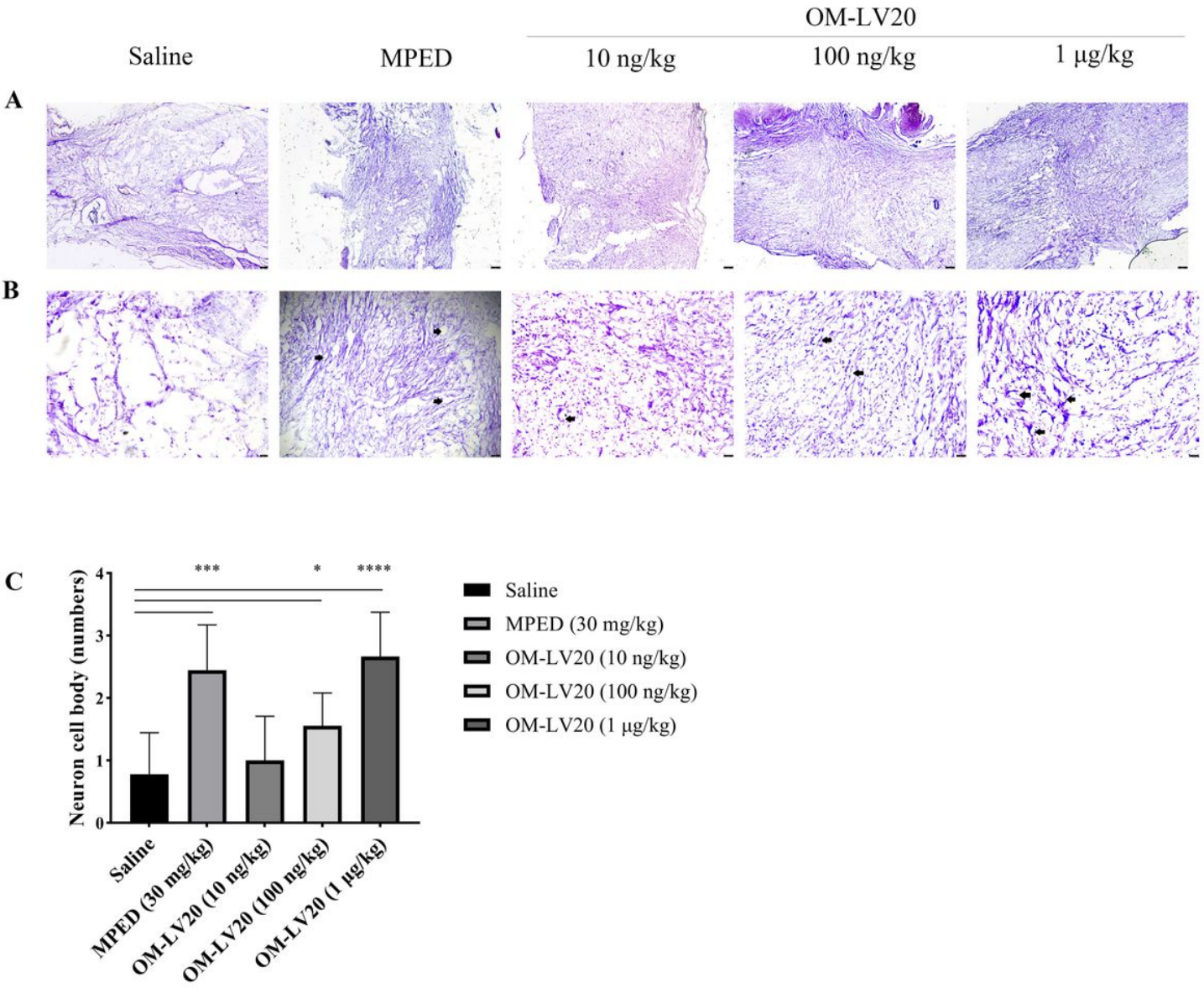

Figure 6

Immunohistochemical and ELISA analysis of BDNF expression 4 weeks after surgery. A. The samples were observed at 10 × field-of-view magnification. Scale bar, 25 μm. B. Quantification of BDNF based on immunohistochemical staining. C. Quantification of BDNF based on ELISA. * Significant difffference at $p < 0.05$; **** $p < 0.0001$. All bars represent means ± SD from three difffferent sections for each experiment.

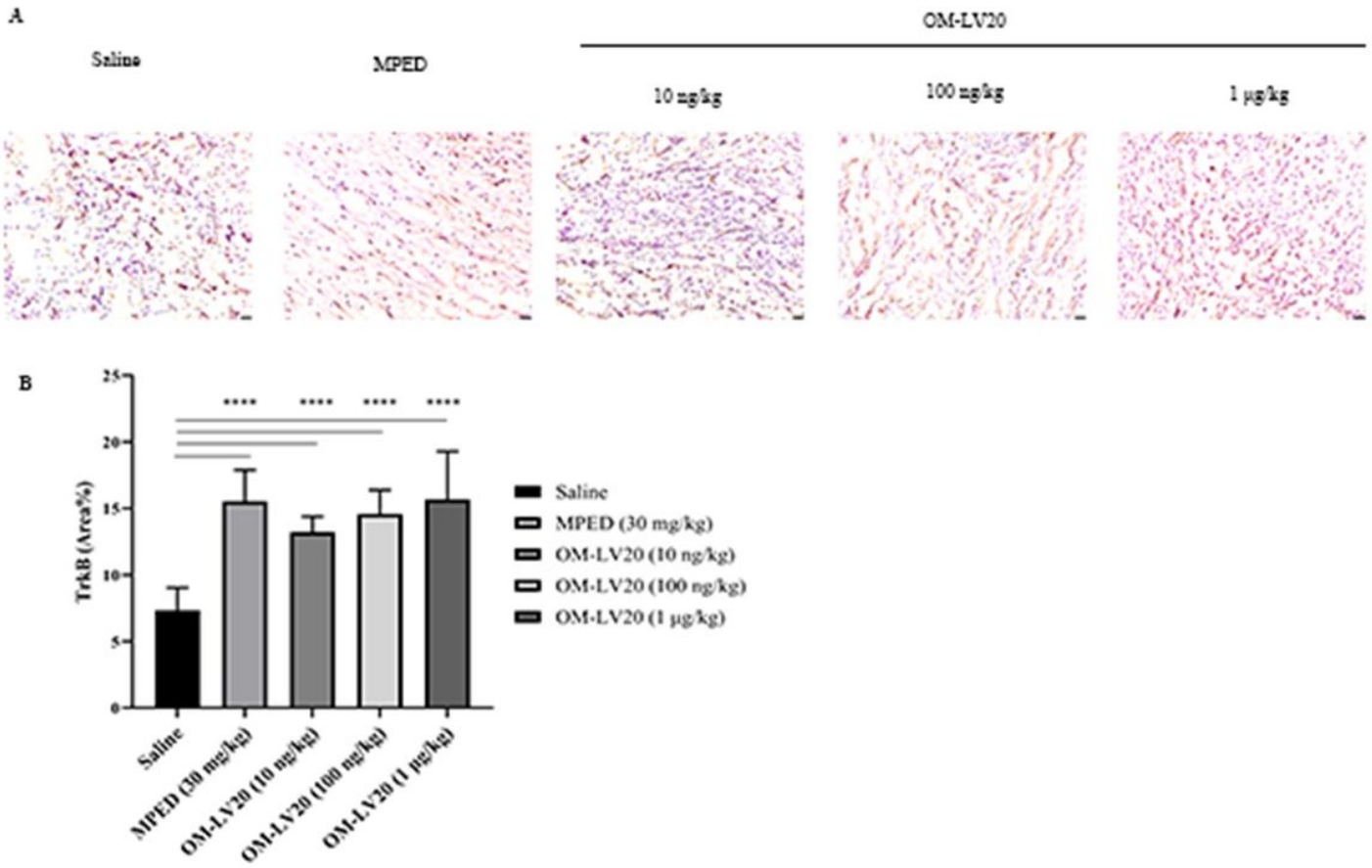

Figure 7

Immunohistochemical analysis of TrkB expression 4 weeks after surgery. A. The samples were observed at 100 ×field-of-view magnification. Scale bar, 25 μm. B. Quantification of TrkB based on immunohistochemical staining. **** Signifificant difffference at $p < 0.0001$. All bars represent means ± SD from three diffferent sections for each experiment.

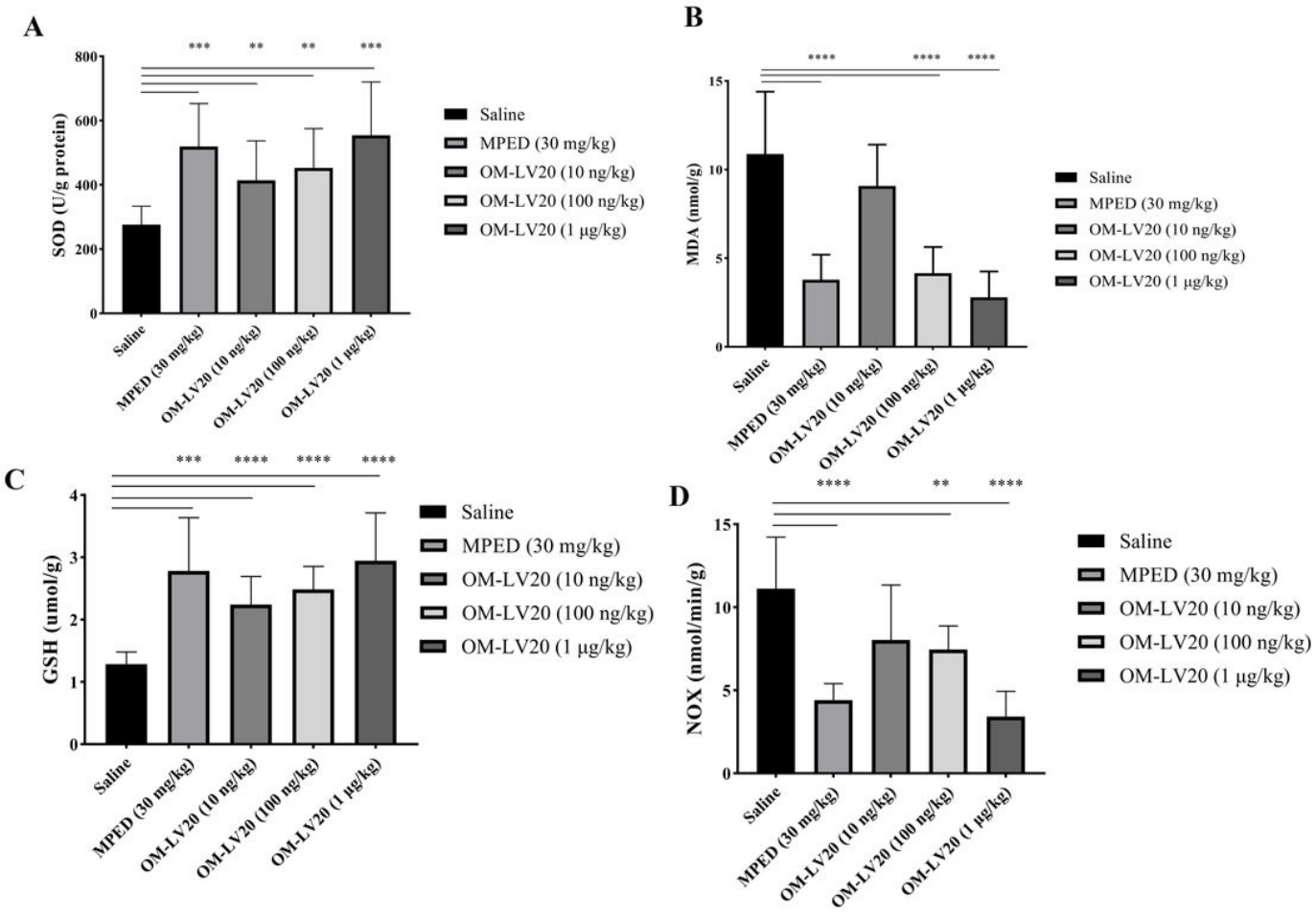

Figure 8

Quantification of biochemical detection indices in spinal cord (between L-2 and L-5) 48 h after surgery. A. SOD content. B. MDA content. C. GSH content. D. NOx content . ** Significant difffference at $p < 0.01$; ***$p < 0.001$; **** $p < 0.0001$. All bars represent means ± SD from three diffferent sections for each experiment.